COLOR ESTIMATION UNDER POISSON NOISE

H. J. Trussell

Dept of Electrical and Computer Engineering
NC State University
Raleigh, NC 27695-7911

M. J. Vrhel

Artifex Software Inc.
San Rafael, CA 94903

ABSTRACT

The dominance of Poisson noise over signal independent Gaussian noise and other types has been demonstrated for commercial digital color cameras. We present a new method for estimating CIE colorimeric values in the presence of Poisson noise. The new methods use multidimensional look-up tables (MLUTs) and are easily adapted to the local statistics of the image. The methods are shown to perform better than common methods that are based on signal independent noise models.

Index Terms— digital imaging, digital cameras, noise models, color estimation, denoising

1. INTRODUCTION

There have been many applications that use digital cameras for precision measurements. Most are familiar with those in astronomy and space exploration [1] and recording of museum artwork [2, 3, 4]. Common to these applications is the fabrication of a camera or camera system that is designed for the specific application. As digital cameras have improved in both resolution and dynamic range, users have begun to consider using commercial cameras for applications that require accuracy in both spatial resolution and colorimetry. In this paper, we consider the colorimetric requirements of such cameras and introduce methods to better estimate CIE colorimetric values from the device dependent RGB values of the camera. These results are important in such applications as medical imaging, book capture and textile quality control.

In using a commercial camera, we are limited to post-processing of the recorded data. We cannot tamper with the internal hardware of the device. We can perform various tests that will characterize the individual subsystems of the camera. Our goal is to show how to use a commercial camera to obtain colorimetric values at a spatial resolution that is needed for the applications mentioned above.

In order to use a camera to obtain spatially accurate color, we need to consider several aspects of the camera's image capture process. The data capture process depends on the optics that control the focus and uniformity of the image on the sensor, the sensor characteristics that transform the radiant spectral color information to digital values, and the noise characteristics of the analog and digital electronics that distort the recorded image data. The user cannot alter any of these characteristics, but can measure them and adjust the processing to reflect these properties. In this work, we consider the transformation from the device dependent RGB values of the camera to the device independent colorimetric values represented by CIEXYZ or CIELAB,

Our transformation accounts for the dominance of Poisson noise in the image capture process. There has been other work addressing Poisson denoising but not in the context of colorimetric estimation [5, 6, 7]. Some use of color cameras for colorimetric works was done, but they did not consider Poisson noise or local processing [8, 9]. The demosaicking work by Hirakawa and Parks, [10], addresses Poisson noise and color fidelity but in a global sense, using the sCIELAB metric. They assume the sRGB values of the camera are accurate colorimetrically. We develop three algorithms to estimate the colorimetric values. The methods vary from global to local processing and linear to nonlinear transformations. As might be expected, the locally adaptive, nonlinear method performs best.

2. SPATIALLY ACCURATE COLOR

Since cameras record three color channels, it can be regarded as a spectroradiometer. Typical spectroradiometers record the spectrum across the visible range, 390nm to 730nm, at a resolution of 4-10nm. The angle of the single measurement ranges from 2 degrees to as small as 1/8 degree. Finally, the accuracy of the measured value is extremely high due to precision optics and well-calibrated sensor. The instrument is environmentally conditioned to be stable and calibrated with a source traceable to NIST standards.

The camera has the great advantage of recording high resolution images. The angle of the measurement of a single pixel is a small fraction of a degree, 0.005 degree or less. The color fidelity and noise properties are significantly poorer. With only three (or sometimes four) spectral bands, the camera cannot approach the spectral resolution of the spectroradiometer, nor the color accuracy of a dedicated colorimeter. The major problem is that the color filters of the camera do

not allow an accurate transformation to the CIE color space. Finally, the noise associated with the camera sensor is much larger than that of the dedicated device. The radiometer requires longer exposures to achieve the low noise levels, usually a minimum of 5ms, for very bright sources. The camera is designed for higher shutter speeds to stop the movement degradation of images. The cost of faster shutter speed is higher noise, caused by shorter integration times for the exposure and higher amplification of recorded data.

There are three main problems with commercial cameras other than Poisson noise that affect the accuracy of color estimation at the pixel level. These include spatial uniformity, variation of the filters and gains of the individual sensor cells and the dynamic range effects of dealing with images.

Camera optics typically have variability across the focal plane. For applications that require comparison of colorimetric values across the entire frame, this problem is important. For the case of quality control of patterned textile material, this must be accounted for. However, for this work, we will consider only local effects and the spatial nonuniformity is measured as a variation in the luminance of the CIELAB estimation. The correction for nonuniformity can be done after the estimation for colorimetric values.

The second problem is nonuniform response of the individual sensors, called Photo Response NonUniformity (PRNU). This is caused by a variation in the spectral sensitivity of the filter and the electronic gain at an individual pixel. The combination of the two effects is to produce a signal dependent noise whose variance is linear with the square of the mean signal (number of photons). This noise will dominate the photon noise that is linear with the mean of the signal at high intensity, since the proportionality is dependent on the variance of the nonuniformity at the pixel level. In the authors' experience, modern CCD devices are so consistent that this PRNU is not a significant noise factor. Consider the plots of variance vs. mean in [10, 11].

3. COLORIMETRIC ESTIMATION

We present three approaches to color estimation. In all of the approaches, we assume we have a collection of K sample reflectances, $\{\mathbf{r}_k\}_{k=1}^{K}$, that represent an ensemble of interest. The reflectances are $N \times 1$ vectors that represent the reflectances for the wavelengths within the visible range, about 390nm to 730nm. The camera RGB values, $\mathbf{c}$, are obtained by the model

$$\mathbf{c} = \mathbf{S}^T\mathbf{L}\mathbf{r} + \boldsymbol{\eta} \tag{1}$$

where $\mathbf{S}$ is a $N \times 3$ matrix of spectral sensitivities of the red, green and blue sensors in the color filter array; $\mathbf{L}$ is the $N \times N$ diagonal matrix of the recording illuminant; $\boldsymbol{\eta}$ is the 3×1 vector of noise associated with the measurement. The sensitivities of the matrix $\mathbf{S}$ may be obtained by the user with commercially available instruments. The ideal colorimetric value that is desired is given by

$$\mathbf{t} = \mathbf{A}^T\mathbf{L}\mathbf{r} \tag{2}$$

where $\mathbf{A}$ is the $N \times 3$ matrix of the CIE color matching functions. We will combine the illuminant with the sensitivity matrix and the color matching function matrix and drop it from subsequent equations.

A major problem with color estimation is that the sensitivity matrix, $\mathbf{S}$, defines a different 3-dimensional subspace of the N-dimensional space, than does the matrix of CIE color matching functions, $\mathbf{A}$. While the camera manufacturers strive to create filters that produce good color, they are never within a linear transformation of $\mathbf{A}$. For color estimation applications, such as this one, it is important to use the raw data from the camera. Using the camera processed sRGB data from JPEG or TIFF files includes unknown processing that adds error to the final colorimetric estimation.

Using the linear mean square error estimate, the transformation from the measurement to the estimate is given by

$$\hat{\mathbf{t}} = \mathbf{M}\mathbf{c} \tag{3}$$

where

$$\mathbf{M} = E\{\mathbf{t}\mathbf{c}^T\}E\{\mathbf{c}\mathbf{c}^T\}^{-1}\mathbf{c}. \tag{4}$$

Using the fact that the noise for each channel is independent of the reflectances, The estimate can be written

$$\hat{\mathbf{t}} = \mathbf{A}^T\mathbf{R}\mathbf{S}(\mathbf{S}^T\mathbf{R}\mathbf{S} + \boldsymbol{\Lambda})^{-1}\mathbf{c}. \tag{5}$$

where $\mathbf{R}$ is the autocovariance of the reflectances and the $\boldsymbol{\Lambda}$ is the autocovariance of the noise. This estimate is suitable for estimation of the CIEXYZ values, from which the CIELAB values can be obtained by the usual nonlinear transformation.

At this point, we need to discuss the noise matrix associated with the Poisson process. Since the red, green and blue sensors are separate in the typical Bayer color filter array of a camera, the noises in the channels are independent of each other. The variance of a Poisson process is equal to the mean. For an individual measurement, we can write the noise vector as

$$\boldsymbol{\eta} = diag(\mathbf{S}^T\mathbf{r})^{1/2}\boldsymbol{\epsilon}. \tag{6}$$

where we assume the number of photons is large enough to use the Gaussian approximation, the 3×1 vector $\boldsymbol{\epsilon}$ is normal, zero mean, unit variance and the square root of the diagonal matrix is taken on each of the terms. For the estimator, we need

$$\boldsymbol{\Lambda} = E\{diag(\mathbf{S}^T\mathbf{r})^{1/2}\boldsymbol{\epsilon}\boldsymbol{\epsilon}^T diag(\mathbf{S}^T\mathbf{r})^{1/2}\}. \tag{7}$$

Taking the expected value of the independent Gaussian noise, we have

$$\boldsymbol{\Lambda} = E\{diag(\mathbf{S}^T\mathbf{r})\}. \tag{8}$$

where the expectation is over the ensemble of reflectances. Our interpretation of this term is very important.

If we assume that the expectation is over all of the ensemble, it is likely that the elements on the diagonal will be quite similar. This is confirmed in the section of results. It is important to take into account the variation of the Poisson noise over the three R,G,B channels. We will refer to the algorithm using the global expected values as the Global (G) method.

We are trying to estimate the colorimetric vector $\mathbf{t}$ associated with the measured vector $\mathbf{c}$. Since we know the measured values, we can use that knowledge to estimate the relative variability of the noise in the different channels. Instead of using the expected value, $\hat{\mathbf{\Lambda}} = E\{diag(\mathbf{S}^T\mathbf{r})\}$, we can use $\hat{\mathbf{\Lambda}} = diag(\mathbf{c})$. This has the advantage of using a better estimate for local areas of the image. For example, areas that are basically yellow would have higher noise variances in the red and green channels and lower variance in the blue channel. The inaccuracy caused by the measurement noise is much less than that caused by averaging over the entire ensemble.

An additional gain in accuracy can be obtained, but at a higher cost, by estimating the covariance matrix $\mathbf{R}$ locally, rather than globally. This can be done by estimating $\mathbf{R}$ by using only the sample reflectances, $\mathbf{r}_k$, that produce vectors $\mathbf{S}^T\mathbf{r_k}$ within a small distance of $\mathbf{c}$. We will refer to the algorithm using the local expected values of noise and covariance as the Local (L) method.

To implement this adaptive method effectively for camera data, we use a multidimensional look-up table (MLUT). The values $\mathbf{t}$ at the grid points $\mathbf{c}$ of the table are determined using Eq.(5) with local statistics from the sample data. We use trilinear interpolation within the MLUT. This enables us to account for variations in the noise level as a function of signal level as well as account for spectral correlation differences in different parts of the camera RGB color space.

When creating the MLUT, the values at grid points in the interior of the training samples are determined using samples that include the grid point in their convex hull. For this case, we use from four to eight samples, depending on their proximity. For the remaining grid points, we obtain the local statistics from the 10 closest (in RGB Euclidean distance) training samples. This number of samples was obtained through empirical testing.

For colorimetric accuracy, we actually desire to minimize the color error in a perceptually uniform color space such as CIELAB or CIECAM02. Finding an optimal transformation to map from camera RGB to CIELAB that minimizes ΔE_{ab} requires the use of numerical methods to find the parameters of a nonlinear function. We will restrict ourselves to finding the optimal matrix $\mathbf{M}$ of Eq. (3) that minimizes the perceptual error. The problem can be posed as find the matrix $\mathbf{N}$ that minimizes

$$||\mathcal{F}(\mathbf{N}\mathbf{S}^T\mathbf{r}) - \mathcal{F}(\mathbf{A}^T\mathbf{r})||^2 \quad (9)$$

where $\mathcal{F}$ is the mapping from CIEXYZ to the perceptually uniform color space. This problem can be posed to find a global matrix that is optimal for the entire data set, or one can construct an MLUT that accounts for local statistics of the sample data, where a number of these problems are solved for MLUT grid points. Since the global approach was seen to give poor results, we concentrate on the local method. We use the same local training samples as in the Local (L) method. We refer to this method as Local Perceptual (LP).

The Local method could easily include the effects of signal-dependent noise by using the noise covariance matrix $\hat{\mathbf{\Lambda}} = diag(\mathbf{c})$. The numerical optimization methods do not permit such easy inclusion. We could include the effects of noise by generating samples $\mathbf{c}$ for each $\mathbf{t}$ that contained different realizations of the noise. While we are considering this approach, at this time, the increase on the number of sample points in the numerical algorithm makes the computational time prohibitive. Thus, for this method, we use use an optimized MLUT based on noiseless data. We will see in the following section how this is affected by measurement noise.

4. RESULTS

To compare the performance of the methods, we used the set of over 2000 reflectance spectra obtained by [12] as a training data set. We used spectral samples from the 140 sample X-Rite ColorChecker Digital SG Chart to test performance [13]. We used the training set to compute the global and local expected values for the Global (G) Local (L) and Local Perceptual (LP) methods. The local methods were implemented using a 17x17x17 MLUT. Across the entire data set, with signal dependent noise, the relative noise variances in the red, green and blue channels as given by Equation 8 is found to be $\mathrm{diag}[1.0, 0.87, 0.81]$. This variance reflects the raw data. The relative values depend on the density of the red, green and blue filters of the Bayer array.

To compute the performance metrics, we trained the methods using simulated data according to the model of Eq.(1), where the noise is Poisson, the illuminant is D50, and the camera spectral sensitivities are as shown in Fig. (1). In the first case, the optimal transforms were found where there was no noise assumed to be present in the system. This provides an optimal benchmark with which to compare the inclusion of the effects of noise in the estimation. To test the degradation of the methods in the presence of noise, we run the noiseless estimators with data contaminated by noise at 25dB, 35dB and 45dB SNRs for the testing and training data. We used the average over the entire ensemble to compute the SNR, noting that the SNR is necessarily signal dependent. The results are shown in Table 1. The errors for the noisy cases, were averaged over 100 realizations for each reflectance vector. The error metrics in the table are the Euclidean distance in CIEXYZ color space (ΔXYZ,) the average color difference ΔE_{ab} in CIELAB space (shown as ΔE in the table to save space), as well as the maximum ΔE_{ab} value found across the tested noise realizations. We note that all methods degrade similarly with decreasing SNR and there is a major drop in performance between 35 and 25dB SNR.

The Local Preceptive method performs best except at the highest noise level.

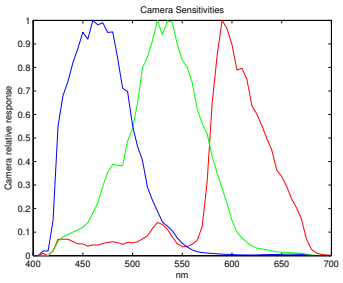

Fig. 1. Spectral sensitivities used for simulation

To determine the effects of considering the noise in the estimation algorithm, optimal transforms that minimized mean squared error in CIEXYZ color space for average signal-dependent noise levels of 25dB, 35dB and 45dB SNR were determined. The results using these transforms with and without noise for the testing and training data are provided in Tables 2-4. The Local Perceptual method is not included in these tables, since it was not modified to account for noisy data.

Comparing the Δ XYZ values between Table 1 and Tables 2-4, we see that knowledge about the signal dependent nature of the Poisson noise can be useful in reducing the estimation error, slightly at higher SNRs and more effectively at the lowest SNR. The estimators that are designed to account for noise perform better in the presence of noise those that are optimal for the noise free case, especially for the ΔE_{max}, e.g., compare 35, 25 dB. In particular, note the lower error for both the Testing and Training data for the Local Method, which should be expected. We see that the optimal Δ XYZ estimators actually do not perform too poorly in terms of ΔE_{ab} compared to the optimal estimators that actually minimize ΔE_{ab}.

An interesting observation is that the Local Perceptual method outperforms the Local method at all but the lowest SNR. This indicates that if the actual noise in the camera is sufficiently small, ignoring it may not be very detrimental. It also hints that developing the LP method to account for noise would be helpful for low SNRs. Images that show the color errors are found at ftp://ftp.eos.ncsu.edu/pub/eos/pub/spectra/.

5. CONCLUSIONS

We have demonstrated that accounting for Poisson noise is helpful, especially at lower SNRs. Locally adaptive methods clearly outperform global methods, as expected. Furthermore, the MLUT approach appears to be viable for optimizing locally adaptive algorithms.

The authors would like to thank Dietmar Wueller for providing access to his data base of spectral radiant measurements.

SNR	Data Set	Method	ΔXYZ	ΔE	ΔE_{max}
25dB	Train	G	5.96	7.54	71.58
		L	5.99	7.56	52.50
		LP	5.93	7.40	60.88
	Test	G	12.05	8.35	66.29
		L	11.21	8.14	49.97
		LP	11.92	8.43	64.68
35dB	Train	G	1.12	2.72	37.29
		L	0.94	2.67	19.14
		LP	0.93	2.47	20.25
	Test	G	4.33	4.80	35.80
		L	3.03	4.18	24.10
		LP	3.36	4.14	19.98
45dB	Train	G	0.64	1.39	30.53
		L	0.43	1.45	11.09
		LP	0.44	1.10	9.28
	Test	G	3.52	4.15	21.66
		L	2.21	3.44	14.39
		LP	2.54	3.40	15.54
No Noise	Train	G	0.58	1.05	26.82
		L	0.37	1.22	7.99
		LP	0.38	0.78	7.06
	Test	G	3.43	4.06	17.95
		L	2.11	3.33	11.52
		LP	2.46	3.29	13.08

Table 1: Optimal Δ XYZ estimators (G and L) and optimal ΔE estimator (LP) for noise free case

SNR	Data Set	Method	ΔXYZ	ΔE	ΔE_{max}
45dB	Train Data	G	0.64	1.39	29.78
		L	0.43	1.44	11.00
	Test Data	G	3.51	4.17	20.19
		L	2.21	3.48	13.53
No Noise	Train Data	G	0.58	1.05	26.97
		L	0.37	1.23	8.37
	Test Data	G	3.43	4.07	17.55
		L	2.11	3.37	11.42

Table 2: Optimal Δ XYZ estimator for 45dB SNR

SNR	Data Set	Method	ΔXYZ	ΔE	ΔE_{max}
35dB	Train Data	G	1.12	2.69	39.35
		L	0.91	2.71	18.36
	Test Data	G	4.29	4.91	23.62
		L	3.01	4.47	18.32
No Noise	Train Data	G	0.59	1.07	28.20
		L	0.40	1.56	9.06
	Test Data	G	3.45	4.22	14.26
		L	2.22	3.83	11.36

Table 3: Optimal Δ XYZ estimator for 35dB SNR

SNR	Data Set	Method	ΔXYZ	ΔE	ΔE_{max}
25dB	Train Data	G	5.52	6.70	65.96
		L	5.38	6.77	56.19
	Test Data	G	11.87	9.17	53.24
		L	10.47	8.49	34.96
No Noise	Train Data	G	1.08	2.52	36.18
		L	0.88	2.84	20.73
	Test Data	G	5.03	6.53	22.93
		L	3.85	6.09	25.63

Table 4: Optimal Δ XYZ estimator for 25dB SNR

6. REFERENCES

[1] website lists many documents describing Hubble Space Telescope imaging, http://www.stsci.edu//hst//HST_overview//documents

[2] K. Martinez, J. Cupitt, D. Saunders,and R. Pillay, " Ten Years of Art Imaging Research," Proc. IEEE Vol. 90, No. 1, pp. 28-41, Jan. 2002.

[3] H. Maitre, F. Schmitt, and C. Lahanier, " 15 years of image processing and the fine arts," Proc. IEEE Int. Conf. on Image Processing, Vol. 1, pp. 557-561, Thessaloniki, Greece, Oct. 2001

[4] A. Ribes, F. Schmitt, R. Pillay, C. Lahanier, " Calibration and spectral reconstruction for CRISATEL : An art painting multispectral acquisition system," J. Imaging Science and Technology, Vol. 49, No. 6, pp 563-573, 2005.

[5] H. Faraji, W. J. MacLean, " CCD Noise Removal in Digital Images," IEEE Trans. Image Proc., Vol. 15, No. 9, pp. 2676-2685, Sept. 2006.

[6] F-X Dupe, J. M. Fadil and J-L. Starck, " A proximal iteration for deconvolving poisson noisy images using sparse representations," IEEE Trans. Image Proc., Vol. 18, No. 2, pp. 310-321, Feb. 2009.

[7] S. Lefkimmiatis, P. Maragos and G. Papandreou, " Baysian inference on multiscale models for Poisson intensity estimation: applications to photon limited image denoising," IEEE Trans. Image Proc., Vol. 18, No. 8, pp. 1724-1741, Aug. 2009.

[8] W. Wu, J. P. Allebach and M. Analoui, "Imaging colorimetry using a digital camera," J. Imaging Science and Technology, Volume 44, Number 4, July/August 2000.

[9] D. Y. Ng, J. P. Allebach, M. Analoui, and Z. Pizlo, " Noncontact imaging colorimeter for human tooth color assessment using a digital camera," J. Imaging Science and Technology, Volume 47, Number 6, November/December 2003.

[10] K. Hirakawa and T. W. Parks, " Joint Demosaicing and Denoising," IEEE Trans. Image Proc., Vol. 15, No. 8, pp. 2146-2157, Aug. 2006.

[11] H. J. Trussell and R. Zhang, "Dominance of Poisson Noise in Color Digital Cameras," IEEE International Conf. on Image Proc., 30 Sept. - 3 Oct. 2012, Orlando, FL.

[12] D. Wueller, "In Situ Measured Spectral Radiation of Natural Objects," Seventeenth Color Imaging Conference: Color Science and Engineering Systems, Technologies, and Applications Albuquerque, New Mexico, pp. 159-163, Nov. 2009.

[13] http://xritephoto.com/ph_product_overview.aspx?id=938&catid=28